Sakarya University Journal of Science 25(4), 926-937, 2021

Buck-type Single-phase AC-AC Active Tracking Voltage Regulator Controlled by an Enhanced Hybrid Control Method

Faruk YALÇIN*[1], Felix HIMMELSTOSS[2]

Abstract

In this paper, a single-phase switch-mode buck-type AC-AC voltage regulator is presented with reduced numbers of elements which are used in the topology. Apart from similar studies in the literature, a new hybrid control method which is structured by the closed-loop PID controller and a new enhanced feedforward controller is used for the control of the regulator. The hybrid controller improves the active tracking capability of the reference to achieve an output voltage as close to the sine-wave with high quality. The input AC voltage may be an ideal sine wave or it may include harmonics. Both simulation and experimental tests are applied for the proposed regulator controlled by this control method. The experimental set-up for the regulator is designed for 0-200 Vp input voltage (50 Hz), 0-100 Vp output voltage, and 0.6 kW output power. The results proved the capability of the proposed buck-type switch-mode regulator to achieve the requested output voltage as near as possible to sine wave. The obtained output voltages for different load conditions and input-output parameters have less than 5% THD (total harmonic distortion) and high quality.

Keywords: AC-AC regulator, active tracking, buck converter, single-phase, harmonics

1. INTRODUCTION

Increasing demand for electrical power causes many problems in power systems such as decreasing power quality for the AC consumers. AC devices must be supplied by an alternating supply voltage between a magnitude band that is generally very narrow for most of the sensitive devices. Various loadings in the distribution systems effect voltage sags/swells which are the main quality problem for the AC consumers. Also in some specific applications, some AC consumers require adjustable voltage magnitudes different to the network voltage levels. Thus, AC voltage regulation becomes so important, that studies are published in increasing number.

The regulation of voltage variations can be provided by the FACTS devices, such as voltage sag supporters [1,2], DVRs (dynamic voltage restorers) [3,4], voltage sag/swell compensators [5,6], and voltage conditioners [7,8] in distribution systems. The mentioned devices provide voltage regulation of the distribution line

* Corresponding author: farukyalcin@sakarya.edu.tr
[1] Sakarya University Of Applied Sciences, Faculty Of Technology, Department Of Mechatronics Engineering, Sakarya, Turkey.
ORCID: https://orcid.org/0000-0003-2672-216X
[2] Fachhochschule Technikum Wien, Höchstädtplatz 6, 1200 Wien.
E-Mail: felix.himmelstoss@technikum-wien.at
ORCID: https://orcid.org/0000-0001-8482-2295

to reach the desired network voltage levels. In this way, supply of the AC consumers which are connected to the distribution buses by the determined network voltages is provided. Thus, individual voltage regulation of each independent AC consumer cannot be possible in this way. On the other hand, these regulators based on FACTS devices require a coupling transformer in addition to a VSI (voltage source inverter). The VSIs, which are incorporated into the mentioned FACTS devices-based regulators, can be structured by either an AC-DC-AC converter or a DC-AC converter. VSIs based on a DC-AC converter demand capacitors and batteries which are independent external DC storage systems. Thus, robust compensation of voltage sags/swells cannot be provided by VSIs based on a DC-AC converter for long terms. Besides, the capabilities of the compensation are limited because of the external storage unit capacities. AC-DC-AC converter-based VSIs do not require any external storage systems, because these converters include an AC-DC structure in the converter topologies. Despite the mentioned advantage of AC-DC-AC converters, additional AC-DC sub-units cause increased losses of the FACTS devices.

Voltage regulation of AC consumers can be provided by standalone AC-DC-AC based VSIs mentioned above instead of using the FACTS-based voltage regulators [9,10]. On the other hand, individual voltage regulation of each AC consumer can be achieved from the constant distribution voltage level in this way. But, the AC-DC stage of these VSIs causes loss increase of the complete AC-AC conversion.

As mentioned above, direct VSI applications and the FACTS devices-based regulators have disadvantages and complexity problems. So, the direct AC-AC conversion method becomes the best solution. For this aim, various kinds of direct AC-AC regulators are studied in the literature. PWM-based traditional AC-AC choppers emerge as the simple and basic solution for the AC-AC regulation [11]. But these AC regulators cause high-level harmonics at the output, because of the chopping structure of the input sine-wave. Thus, these chopper regulators require additional filtering units, such as coupling transformers or passive filters. Buck [12-14], boost [15,16], and buck-boost [17,18] type switch-mode AC-AC regulators are studied increasingly for AC regulation in the literature in recent years. These switch-mode regulators do not need additional filtering units as in PWM AC choppers because of the switch-mode operation. Thus, obtaining close to sine wave output voltages with low THD can be achieved. These regulators have also a lower complex topology. The mentioned switch-mode AC-AC regulators are applied successfully to the AC regulation applications in the literature. But these studies have the lack that applying input AC voltages including harmonics is absent in these studies. In the literature, the existing similar studies consider pure sine-wave input AC voltages. But, many AC consumers may be supplied with non-sinusoidal voltages with different harmonics because of various distortions in application and in the mains. So, harmonic elimination capability of an AC-AC regulator is required in addition to the AC voltage regulation capability. According to the standards, supplying of the AC customers through high-quality AC voltages with THD less than 5% is so important [19].

In this study, a single-phase buck-type active tracking AC-AC voltage regulator is presented. Also, an improved control method is proposed for the active tracking of the desired reference output sine-wave. The presented topology (and other ones) of the regulator and the control method are patented by the co-author of this study [20]. The presented topology of the regulator incorporates moderate numbers of components, just one inductor, one capacitor, and four active switches. The buck-type structure of the presented regulator enables the achievement of a wide range of output voltage amplitude lower than the input voltage amplitude. Apart from similar studies in the literature, the proposed control method is a novel hybrid control method composed of a closed-loop PID controller and a new feedforward controller. By this way, active tracking of the reference sine-wave output voltage is improved to achieve nearly close to sine-wave output voltage in the case that the input voltage is a pure sine or not. The presented regulator and control method is tested by both simulation and experimental studies. The

obtained results demonstrate that the proposed buck type switch-mode regulator has the ability of achieving the requested output voltage with reduced harmonics under 5% THD for different load conditions and input-output parameters.

2. THE PROPOSED SINGLE-PHASE BUCK AC-AC REGULATOR

This section describes the proposed buck-type single-phase AC-AC regulator topology, as well as the regulator's operation procedure and dynamic analysis.

2.1. The Regulator Topology

Figure 1 depicts the main circuit of the proposed buck-type single-phase AC-AC regulator [20].

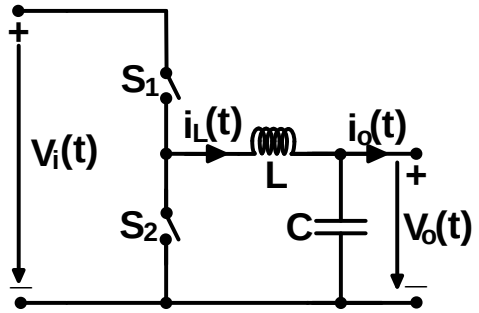

Figure 1 General topology of the proposed buck-type single-phase AC-AC regulator

V_i, V_o, L, and C represent input AC voltage, output AC voltage, inductor and capacitor, respectively in Figure 1. S_1 and S_2 are the bidirectional active switches. These bidirectional active switches are realized by MOSFETs in this study. Thus, the proposed regulator circuit with MOSFETs can be shown in Figure 2.

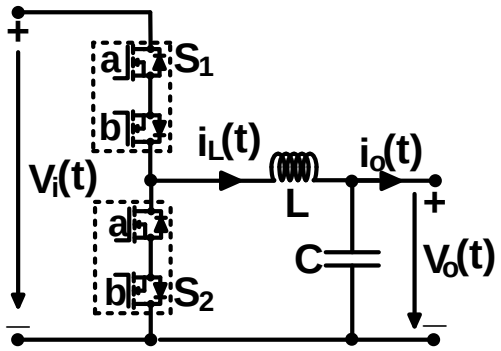

Figure 2 The proposed buck-type single-phase AC-AC regulator with MOSFETs

2.2. The Regulator Operation Procedure

The proposed single-phase AC-AC regulator's operation is based on the well-known conventional buck converter. Instant input voltage $V_i(t)$ is bucked as $V_o(t)$ at the output depending on the control of PWM duty ratio (d) for S_1. Thus, the output voltage is obtained as an AC voltage with the same polarity as the input voltage, but with lower amplitude value than at the input. S_2 acts as supplementary switch of S_1. S_2 is turned off when S_1 is turned on. In this stage, V_i supplies the inductor, the capacitor and the output load. S_2 is turned on when S_1 is turned off. In this stage, the pre-energized inductor supplies both the capacitor and the output load.

The polarity of V_i changes in each half period, because the input voltage V_i is an alternating voltage. So, the on-off states of the sub-active switches of the bidirectional active switches S_1 and S_2 change for each half-period of the input voltage depending on the polarity. The control of the active switches S_1 and S_2 is summarized in Table 1.

Table 1 Control signal of MOSFETs used in Figure 2 as part of the bidirectional active switches S_1 and S_2

State	S_1				S_2			
	Positive Half-Wave Stage		Negative Half-Wave Stage		Positive Half-Wave Stage		Negative Half-Wave Stage	
	S_{1a}	S_{1b}	S_{1a}	S_{1b}	S_{2a}	S_{2b}	S_{2a}	S_{2b}
ON	on	off	off	on	off	on	on	off
OFF	off	off	off	off	off	off	off	off

The MOSFETs' switching pattern can be seen in Figure 3.

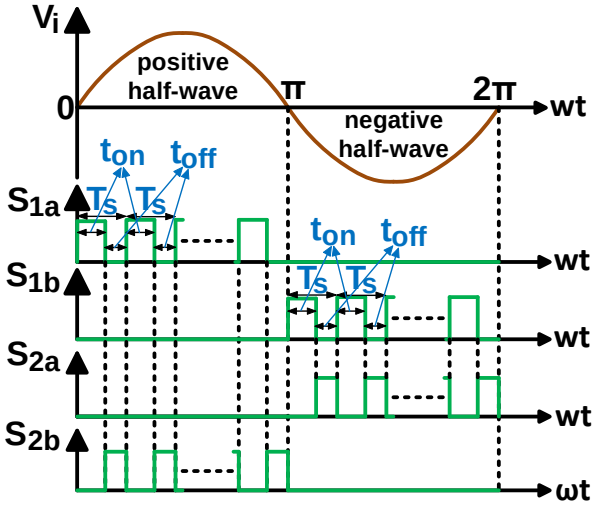

Figure 3 The switching pattern of the MOSFETs

In Figure 4, the equivalent sub-circuits of the proposed regulator topology, which is shown in Figure 2, are given according to the proper control of the mentioned active switches for one cycle sine-wave input voltage.

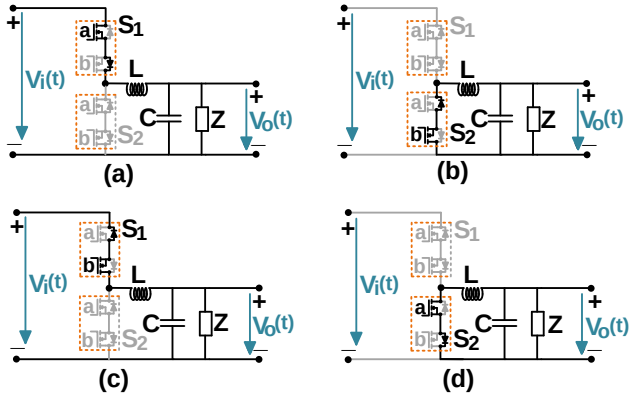

Figure 4 The equivalent sub-circuits of the proposed buck-type regulator *(a) Positive half-wave output stage, on mode (S_1 is on, S_2 is off), (b) Positive half-wave output stage, off mode (S_1 is off, S_2 is on), (c) Negative half-wave output stage, on mode (S_1 is on, S_2 is off), (d) Negative half-wave output stage, off mode (S_1 is off, S_2 is on)*

Thus, producing of the output voltage for one cycle in the proposed regulator operation can be summarized in two main stages by Figure 3 and Figure 4 as follows.

Stage 1 ($0 \leq wt < \pi$): Input AC voltage is in the positive half-wave in this stage. While the PWM on-stage of S_1 (S_2 is off), S_{1a} is turned on, S_{1b} is turned off and both S_{2a} and S_{2b} are turned off. While the PWM off-stage of S_1 (S_2 is on), both S_{1a} and S_{1b} are turned off, S_{2a} is turned off, and S_{2b} is turned on. The desired positive half sine-wave output voltage is produced by the input voltage based on the continuous proper control of d, which is the PWM duty ratio of S_1.

Stage 2 ($\pi \leq wt < 2\pi$): Input AC voltage is in the negative half-wave in this stage. While the PWM on-stage of S_1 (S_2 is off), S_{1b} is turned on, S_{1a} is turned off and both S_{2a} and S_{2b} are turned off. While the PWM off-stage of S_1 (S_2 is on), both S_{1a} and S_{1b} are turned off, S_{2a} is turned on, and S_{2b} is turned off. The desired negative half sine-wave output voltage is produced from the input voltage based on the continuous proper control of d, which is the PWM duty ratio of S_1.

2.3. The Regulator's Dynamic Analysis

In this section, the detailed dynamic analysis of the proposed buck-type single-phase AC-AC regulator is presented. In order to provide reliable analysis for real-time applications, real parasitic effects of the elements used in the topology are taken into account in the analysis.

In Figure 5, the equivalent circuits of the proposed regulator for the positive half-wave input stage are demonstrated. In the given equivalent circuit the selected MOSFETs are identical.

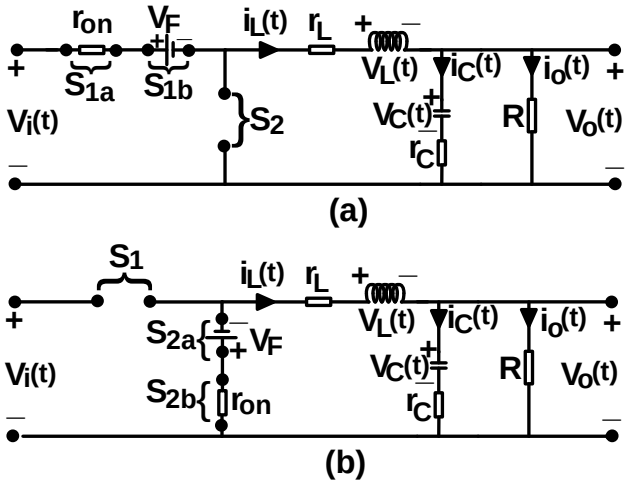

Figure 5 The positive half-wave stage equivalent circuits of the regulator *(a) on-mode – S_1 is turned on and S_2 is turned off, (b) off-mode – S_1 is turned off and S_2 is turned on*

The symbols i_o, i_L, i_C, V_L, V_C, V_F, r_{on}, r_L, r_C, and R represent the output current, inductor current, capacitor current, inductor voltage, capacitor

voltage, forward biasing voltage of the MOSFET's anti-parallel diode, on-resistance of the MOSFET, equivalent series resistance (ESR) of the inductor, ESR of the capacitor, and output load resistance, respectively in Figure 5.

The dynamic analysis of the regulator can be obtained for the positive half-wave input stage from Figure 5. As seen in Figure 5, the dynamic equations for the state variables inductor current and output voltage are obtained for the two modes: on-mode and off-mode.

On-mode (S_1 is on and S_2 is off): For this mode, the state equations for the inductor current and the output voltage can be determined by Figure 5*a*, respectively as below.

$$\frac{di_L(t)}{dt} = -\frac{1}{L}\left(r_L + r_{on}\right)i_L(t) - \frac{1}{L}V_o(t) + \frac{1}{L}\left[V_i(t) - V_F\right] \tag{1}$$

$$\frac{dV_o(t)}{dt} = \frac{R}{R+r_C}\left[\frac{1}{C} - \frac{r_C}{L}\left(r_L + r_{on}\right)\right]i_L(t) - \frac{R}{R+r_C}\left[\frac{r_C}{L} + \frac{1}{RC}\right]V_o(t) + \frac{r_C R}{\left(R+r_C\right)L}\left[V_i(t) - V_F\right] \tag{2}$$

Off-mode (S_1 is off and S_2 is on): For this mode, the state equations for the inductor current and the output voltage can be determined by Figure 5*b*, respectively as below.

$$\frac{di_L(t)}{dt} = -\frac{1}{L}\left(r_L + r_{on}\right)i_L(t) - \frac{1}{L}V_o(t) - \frac{1}{L}V_F \tag{3}$$

$$\frac{dV_o(t)}{dt} = \left(\frac{R}{R+r_C}\right)\left[\frac{1}{C} - \frac{r_C}{L}\left(r_L + r_{on}\right)\right]i_L(t) - \left(\frac{R}{R+r_C}\right)\left(\frac{r_C}{L} + \frac{1}{RC}\right)V_o(t) - \frac{r_C R}{\left(R+r_C\right)L}V_F \tag{4}$$

The state-space model equation of the on-mode can be achieved by (1) and (2) as below,

$$\begin{bmatrix}\dot{i}_L(t)\\ V_o(t)\end{bmatrix} = \begin{bmatrix} -\frac{1}{L}\left(r_L + r_{on}\right) & -\frac{1}{L} \\ \frac{R}{R+r_C}\left[\frac{1}{C} - \frac{r_C}{L}\left(r_L + r_{on}\right)\right] & -\frac{R}{R+r_C}\left[\frac{r_C}{L} + \frac{1}{RC}\right]\end{bmatrix}\begin{bmatrix} i_L(t)\\ V_o(t)\end{bmatrix} + \begin{bmatrix} \frac{1}{L} & -\frac{1}{L} \\ \frac{R}{R+r_C}\frac{r_C}{L} & -\frac{R}{R+r_C}\frac{r_C}{L}\end{bmatrix}\begin{bmatrix} V_i(t)\\ V_F\end{bmatrix} \tag{5}$$

The state-space model equation of the off-mode can be achieved by (3) and (4) as below,

$$\begin{bmatrix}\dot{i}_L(t)\\ V_o(t)\end{bmatrix} = \begin{bmatrix} -\frac{1}{L}\left(r_L + r_{on}\right) & -\frac{1}{L} \\ \frac{R}{R+r_C}\left[\frac{1}{C} - \frac{r_C}{L}\left(r_L + r_{on}\right)\right] & -\frac{R}{R+r_C}\left(\frac{r_C}{L} + \frac{1}{RC}\right)\end{bmatrix}\begin{bmatrix} i_L(t)\\ V_o(t)\end{bmatrix} + \begin{bmatrix} 0 & -\frac{1}{L} \\ 0 & -\frac{R}{R+r_C}\frac{r_C}{L}\end{bmatrix}\begin{bmatrix} V_i(t)\\ V_F\end{bmatrix} \tag{6}$$

The above dynamic analysis is done for an input voltage during the positive half-wave. If a similar dynamic analysis is performed for the negative half-wave, the same state-space equations as given in (5) and (6) are obtained. So, this means that the state-space equations (5) and (6) are valid for both positive and negative half-wave input cases.

Thus, the small signal transfer function between the output voltage and PWM duty ratio can be obtained by (5) and (6) as follows.

$$G_{buck}(s) = \frac{\hat{V}_o(s)}{d(s)} = \frac{gs + \left(ag + cf\right)}{s^2 + \left(a+e\right)s + \left(ae - bc\right)} \tag{7}$$

The coefficients used in (7) are described as follows.

$$a = \frac{\left(r_L + r_{on}\right)}{L} \tag{8}$$

$$b = -\frac{1}{L} \tag{9}$$

$$c = \frac{R}{R + r_C}\left[\frac{1}{C} - \frac{r_C}{L}\left(r_L + r_{on}\right)\right] \quad (10)$$

$$e = \frac{R}{R + r_C}\left[\frac{r_C}{L} + \frac{1}{RC}\right] \quad (11)$$

$$f = \frac{\bar{V}_i}{L} \quad (12)$$

$$g = \frac{r_C R}{\left(R + r_C\right)L}\bar{V}_i \quad (13)$$

In (12)-(13), $\bar{V}_i$ represents the input voltage at the operating point.

3. THE PROPOSED HYBRID CONTROL METHOD

The proposed hybrid control method for controlling the proposed AC-AC regulator is presented in this section. The general control diagram of the proposed regulator is shown in Figure 6.

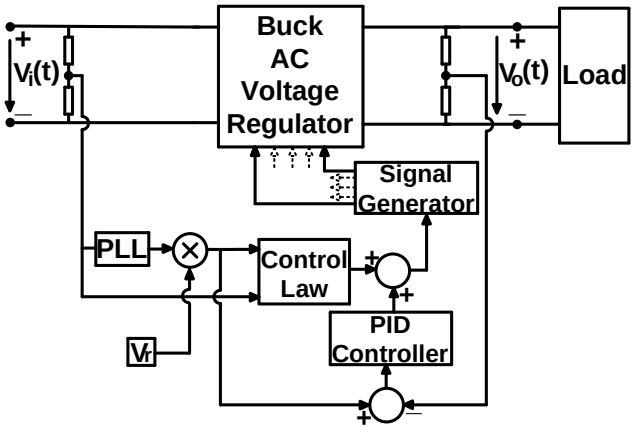

Figure 6 The general control diagram of the proposed regulator

The frequency of the input AC voltage is determined by the PLL, and the magnitude of the reference output AC voltage is described by V_r in Figure 6. Thus, the requested sine-wave reference output voltage can be defined as follows,

$$V_{ref}(wt) = V_r \sin wt \ . \quad (14)$$

The proposed hybrid controller is structured by two main units as seen in Figure 6. One of these units is the traditional closed-loop PID controller. The PID controller eliminates the error between the real output voltage and the reference output voltage, while satisfying the response performance according to the design criteria. The new developed feedforward controller, referred to as "control law (CL)" in Figure 6, is the other component of the hybrid controller. The CL has an open-loop controller structure and produces a PWM duty ratio according to the topology parameters as follows.

$$d_{CL}(wt) = \sqrt{\frac{2L\left|V_r \sin wt\right|\left(\left|V_r \sin wt\right| + V_F\right)}{\left|V_i(wt)\right|\left(\left|V_i(wt)\right| - \left|V_r \sin wt\right| - V_F\right)T_S R}} \quad (15)$$

In (15), T_S defines the PWM switching period. The PWM duty ratio produced by the CL as in (15) cannot directly provide the desired PWM duty ratio for achieving the reference output voltage. However, it will generate a duty ratio that is close to the actual one. As shown in (15), the duty ratio generated by the CL has a static structure which can be produced in a fast manner. Thus, the PID controller is supported by the CL to achieve the desired operating duty ratio with an improved response performance. Thus, the proposed hybrid control method ensures efficient and accurate active tracking of the reference output voltage to achieve sine-wave output voltage as close as possible and with low THD. Consequently, the desired operating PWM duty ratio is achieved by the PID controller and the CL which are part of the hybrid control method as follows.

$$d(wt) = d_{PID}(wt) + d_{CL}(wt) \quad (16)$$

In this paper, discrete-time control is selected for the control of the regulator operation. Thus, the regulator's control block diagram based on the proposed hybrid control method can be demonstrated in Figure 7.

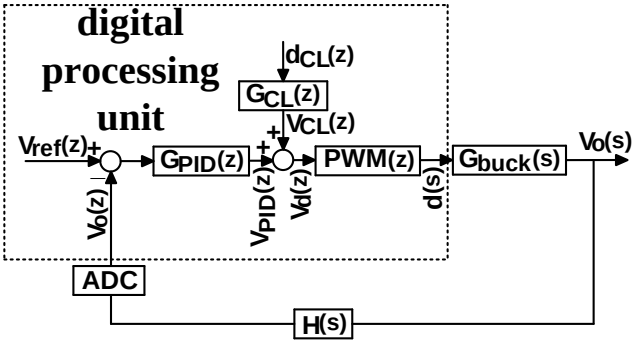

Figure 7 The discrete-time control block diagram based on the proposed hybrid control technique for the buck-type regulator

The relations between the control signals and the transfer functions of the discrete time control block diagram can be derived from Figure 7 as follow.

$$G_{CL}(z) = \frac{1}{PWM(z)} \tag{17}$$

$$V_d(z) = V_{CL}(z) + V_{PID}(z) \tag{18}$$

$$d(z) = V_d(z).PWM(z) \tag{19}$$

The transfer function of the discrete PID controller is defined in this paper as below,

$$G_{PID}(z) = K_P + K_I \frac{z}{z-1} + K_D \frac{z-1}{z} \tag{20}$$

4. THE RESULTS OF THE STUDY

In this section, the design steps, the simulation test results and the experimental test results of the proposed regulator study are presented.

4.1. The Design Parameters of the Regulator Circuit and the Control Method

A laboratory set-up is built for the proposed regulator's real-time experimental application. The set-up is designed for 0-200 Vp input voltage (50 Hz), 0-100 Vp output voltage, and 0.6 kW output power. IXFK98N50P3 type n-channel, high-speed, low on-resistance MOSFETs (V_{DSS}=500 V, r_{on}=50 mΩ, I_D=98 A, V_F=1.5 V) are selected for the active switches in the set-up topology. The values of the switching frequency, the inductor and the capacitor for the regulator circuit are determined as given in Table 2.

Table 2 The selected values of the capacitor, inductor and switching frequency

Switching Frequency f_s (kHz)	Capacitor		Inductor	
	C (μF)	r_C (mΩ)	L (μH)	r_L (mΩ)
50	3.3	180	47	130

The determined operating point parameters which are used for the design of the discrete time PID controller are shown in Table 3.

Table 3 The determined operating point parameters of the regulator operation

$\bar{V}_i$ (V)	$\bar{D}$	$\bar{V}_o$ (V)	R (Ω)
70	0.5	35	50

The parameters of the PID controller defined in (20) are achieved through the design and performance criteria as follows.

$$K_P = -0.124, \quad K_I = 0.052, \quad K_D = 0.0086 \tag{21}$$

4.2. The Simulation Studies

In order to validate the theoretical proposals of the study, simulation tests are applied to the proposed converter with the proposed hybrid control method.

Three different simulation test cases given in Table 4 are applied to the regulator system in MATLAB Simulink. The wave form test results obtained from simulation studies are given in Figures 8-10. The detailed numerical results of the simulation tests for the output are also presented in Table 5. In Table 5, THD_V and THD_I determine the THD values for voltage and current, respectively.

As seen from Figures 8-10 and Table 5, the proposed buck-type single-phase AC-AC regulator can provide the desired reference AC sine-wave voltages as close as possible and with low THD levels under 5% even in the case that the input AC voltages have harmonic components. Thus, both the wave form results in Figures 8-10 and the numerical results in Table 5

prove the accuracy and efficiency of the proposed hybrid control method for the active tracking of the reference output voltages.

Table 4 Test cases for the simulation tests

Test Cases No	Vi	Output Load Z	Desired output fundamental sine-wave voltage V_o (V)
1	120V sine + LOH (f=50Hz)	Resistive R=10Ω	100
2	100V sine + HOH (f=50Hz)	Inductive R=5Ω, L=47mH	80
3	80V sine + fluct. (f=50Hz)	Capacitive R=10Ω, C=1mF	50
fluct.: fluctuations, HOH: high order harmonics, LOH: low order harmonics			

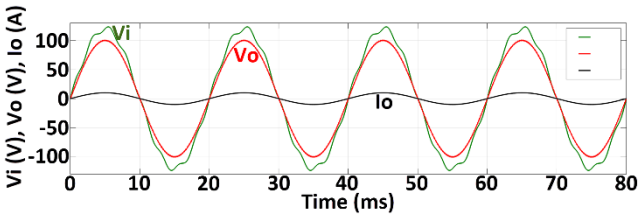

Figure 8 The simulation results for test case-1

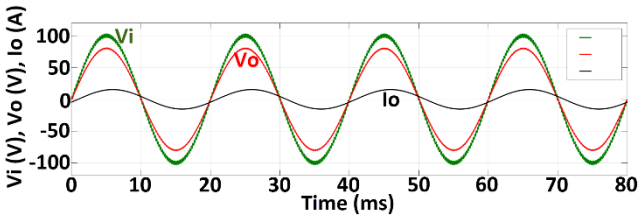

Figure 9 The simulation results for test case-2

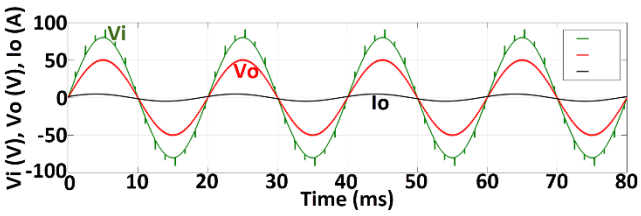

Figure 10 The simulation results for test case-3

Table 5 The obtained numerical simulation results of the test cases

Test Case No	Obtained Fundamental V_o (V)	THD_V (%)	THD_I (%)
1	100.3	2.01	2.01
2	80.2	1.97	1.91
3	50.1	1.99	2.11

4.3. The Experimental Studies

In order to validate the real-time practical application of the study, experimental tests are applied to the proposed AC/AC buck converter with the proposed hybrid control method. The experimental set-up of the regulator system is given in Figure 11.

Figure 11 The built experimental laboratory set-up of the regulator system

Three different experimental test cases given in Table 6 are applied to the experimental set-up of the regulator system. The wave form test results obtained from experimental studies are given in Figures 12-14. The detailed numerical results of the experimental tests for the output are also presented in Table 7.

As seen from Figures 12-14 and Table 7, the proposed buck-type single-phase AC-AC regulator can provide the desired reference AC sine-wave voltages experimentally as close as possible with low THD levels under 5%. Thus, both the wave form results in Figures 12-14 and the numerical results in Table 7 prove the accuracy and efficiency of the proposed hybrid control method for the active tracking of the reference output voltages in experiment.

Table 6 Test cases for the experimental tests

Test Cases No	V_i	Output Load-Z	Desired output fundamental sine-wave voltage-V_o (V)
1	100V sine (f=50Hz)	Resistive R=15Ω	70
2	70V sine (f=50Hz)	Inductive R=25Ω, L=10mH	55
3	85V sine (f=50Hz)	Capacitive R=20Ω, C=0.33mF	40

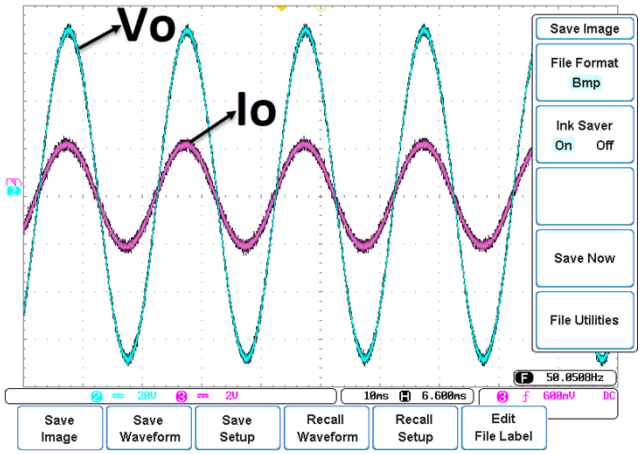

Figure 12 The experimental results for test case-1 (V/div=A/div for I_o)

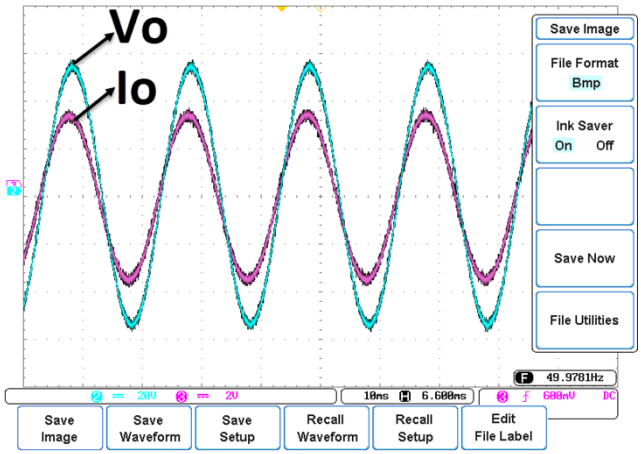

Figure 13 The experimental results for test case-2 (V/div=A/div for I_o)

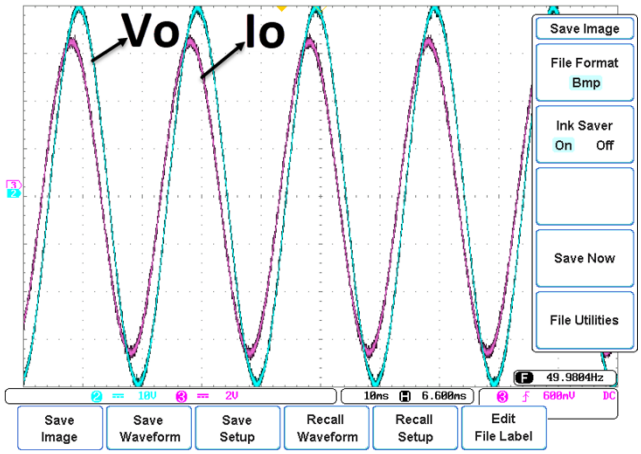

Figure 14 The experimental results for test case-3 (V/div=A/div for I_o)

Table 7 The obtained numerical experimental results of the test cases

Test Case No	Obtained Fundamental V_o (V)	THD_V (%)	THD_I (%)
1	69.8	2.19	2.15
2	55.2	2.14	2.06
3	40.1	2.08	2.21

In order to prove the efficiency of the proposed hybrid control technique for active tracking of the reference output voltage, a comparative test study is performed. In this comparative test study, the proposed hybrid control technique and the standalone PID control are applied to the proposed regulator separately for the experimental test case-2. The achieved output voltage waveforms for the mentioned two separate applications are shown together in Figure 15. The comparative numerical output THD results of the mentioned test cases are also given in Table 8.

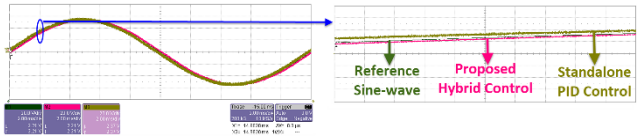

Figure 15 Comparative output voltage V_o wave form of the proposed hybrid control and the standalone PID control for test case-2 (20V/div, 2ms/div)

As can be seen from Figure 15, active tracking of the reference output sine-wave voltage is provided by the proposed hybrid control technique better than with the traditional PID control. So, this proves that the developed CL supports the PID controller and improves the active tracking capability. The results of the output THD are given in Table 8 also shows the capability of the proposed hybrid control technique to achieve a better sine-wave output voltage with high quality and low THD values lower than 5%.

Table 8 Comparative THD results for the proposed hybrid control and the standalone traditional PID control in the experimental test cases

Test Case No	THD (%) results of the proposed hybrid control method		THD (%) results of the traditional standalone PID control	
	THD_V	THD_I	THD_V	THD_I
1	2.19	2.15	2.31	2.30
2	2.14	2.06	2.27	2.22
3	2.08	2.21	2.22	2.38

The efficiency of the proposed buck-type single-phase regulator is achieved for different output power rates regarding the power rate, which is determined by the design criteria. The regulator's efficiency curve is shown in Figure 16. The proposed regulator provides good enough

efficiency with an average 95%, where the regulator is loaded with above half output loading.

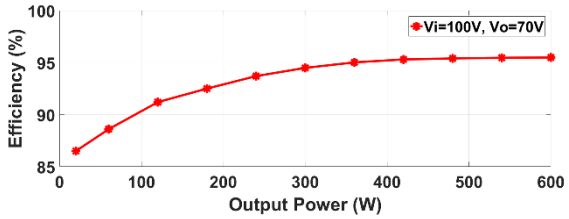

Figure 16 Regulator efficiency curve for different output power rates

5. CONCLUSION

This paper presents a single-phase switch-mode buck-type AC-AC voltage regulator using reduced numbers of elements in the regulator topology. A new hybrid control method composed of a closed-loop PID controller and an enhanced feedforward controller is used for the regulator control, in order to improve the active tracking ability of the reference output voltage to obtain an output voltage as close to the sine-wave with high quality in the case either the input AC voltage is an ideal sine wave or it includes harmonic components. Both simulation and experimental test results prove the ability of the presented switch-mode buck-type regulator to obtain the desired output voltage as close to the ideal sine waveform for different operating conditions with lower than 5% THD.

Acknowledgments

The topology and control theory of the proposed AC regulator in this study are patented by the co-author at the Austrian Patent Office as “Aktive Netzfilter” (patent no: AT 505460 B1, filed 10.07.2007, applied 15.06.2012).

Funding

The authors received no financial support for research and publication of this article.

The Declaration of Conflict of Interest/ Common Interest

No conflict of interest or common interest has been declared by the authors.

Authors' Contribution

The authors contributed equally to the study.

The Declaration of Ethics Committee Approval

The authors declare that this document does not require an ethics committee approval or any special permission.

The Declaration of Research and Publication Ethics

The authors of the paper declare that they comply with the scie The authors of the paper declare that they comply with the scientific, ethical and quotation rules of SAUJS in all processes and declare that Sakarya University Journal of Science and its editorial board have no responsibility for any ethical violations that may be encountered, and that this study has not been evaluated in any academic publication environment other than Sakarya University Journal of Science.

REFERENCES

[1] D. M. Lee, T. G. Habetler, R. G. Harley, T. L. Keister, and J. R. Rostron, “A voltage sag supporter utilizing a PWM-switched autotransformer,” IEEE Transactions on Power Electronics, vol. 22, no. 2, pp. 626–635, 2007.

[2] S. Subramanian and M. K. Mishra, “Interphase AC-AC topology for voltage sag supporter,” IEEE Transactions on Power Electronics, vol. 25, no. 2, pp. 514–518, 2010.

[3] A. Moghassemi and S. Padmanaban, “Dynamic voltage restorer (DVR): a comprehensive review of topologies, power converters, control methods, and modified configurations,” Energies, vol. 13, no. 16, article number: 4152, 2020.

[4] A. AbuHussein and M. A. H. Sadi, “Fault ride-through capability improvement of grid connected PV system using dynamic

voltage restorer," Electric Power Components and Systems, vol. 48, no. 12-13, pp. 1296–1307, 2020.

[5] J. Kaniewski, P. Szczesniak, M. Jarnut, and G. Benysek, "Hybrid voltage sag/swell compensators a review of hybrid AC/AC converters," IEEE Industrial Electronics Magazine, vol. 9, no. 4, pp. 37–48, 2015.

[6] M. K. Nguyen, Y. C. Lim, and J. H. Choi, "Single-phase z-source-based voltage sag/swell compensator," 2013 Twenty-Eighth Annual IEEE Applied Power Electronics Conference and Exposition, pp. 3138–3142, 2013.

[7] H. Hafezi and R. Faranda, "Dynamic voltage conditioner: a new concept for smart low-voltage distribution systems," IEEE Transactions on Power Electronics, vol. 33, no. 9, pp. 7582–7590, 2018.

[8] R. Faranda, A. Bahrami, and H. Hafezi, "Fault current limiting investigation for a single-phase dynamic voltage conditioner," 2019 IEEE Milan Powertech, 2019.

[9] R. Gupta and A. Kumar, "Control of multi-cell AC/DC and cascaded H-bridge DC/AC-based AC/DC/AC converter," IETE Journal of Research, early access, 2020.

[10] P. D. Singh and S. Gao, "Fuzzy based AC-DC-AC converter controlled micro hydro renewable power generation using parallel asynchronous generators for remote areas," International Journal of Renewable Energy Research, vol. 10, no. 1, pp. 260–273, 2020.

[11] K. Venkatesha, H. A. Vidya, R. Sinha, and G. Jayachitra, "Experimental analysis of symmetrical & asymmetrical PWM based single phase AC chopper for power quality improvement using FPGA real time controller," 2017 International Conference On Smart Grids, Power and Advanced Control Engineering, pp. 267–272, 2017.

[12] Y. B. Wang, P. Wang, G. W. Cai, C. Liu, D. B. Guo, H. W. Zhang, and B. D. Zhu, "An improved bipolar-type AC-AC converter topology based on nondifferential dual-buck PWM AC choppers," IEEE Transactions on Power Electronics, vol. 36, no. 4, pp. 4052–4065, 2021.

[13] S. Kim, D. Jang, H. G. Kim, and H. Cha, "Cascaded dual-buck AC-AC converter using coupled inductors," 2018 International Power Electronics Conference, pp. 2619–2624, 2018.

[14] A. A. Khan, H. Cha, J. W. Baek, J. Kim, and J. Cho, "Cascaded dual-buck AC-AC converter with reduced number of inductors," IEEE Transactions on Power Electronics, vol. 32, no. 10, pp. 7509–7520, 2017.

[15] A. Chakraborty, A. Chakrabarti, and P. K. Sadhu, "Analysis of a full-bridge direct AC-AC boost converter based domestic induction heater," Revue Roumaine Des Sciences Techniques - Serie Electrotechnique Et Energetique, vol. 64, no. 3, pp. 223–228, 2019.

[16] H. Sarnago, O. Lucia, A. Mediano, and J. M. Burdio, "Direct AC-AC resonant boost converter for efficient domestic induction heating applications," IEEE Transactions on Power Electronics, vol. 29, no. 3, pp. 1128–1139, 2014.

[17] H. F. Ahmed, H. Cha, A. A. Khan, and H. G. Kim, "A novel buck-boost AC-AC converter with both inverting and noninverting operations and without commutation problem," IEEE Transactions on Power Electronics, vol. 31, no. 6, pp. 4241–4251, 2016.

[18] A. A. Khan and H. Y. Cha, "A novel highly reliable three-phase buck-boost AC-AC converter," 2016 IEEE Energy Conversion Congress and Exposition, 2016.

[19] F. Yalcin, U. Arifoglu, and I. Yazici, "A new single phase inverter based on buck

converter," Sakarya University Journal of Science, vol. 24, no. 3, pp. 480–486, 2020.

[20] F. Himmelstoss, "Aktive Netzfilter," Austrian Patent, patent no: AT 505460 B1, filed 10 July 2007, applied 15 January 2012.